Electronic Supplementary Material (ESI) for Chemical Communications

Electronic supplementary information

A Linear Single-Molecule Magnet Based on $[Ru(CN)_6]^{3-}$

Kasper S. Pedersen,*[a] Jan Dreiser,*[b] Joscha Nehrkorn,[c] Maren Gysler,[c] Magnus Schau-Magnussen,[a] Alexander Schnegg,[d] Karsten Holldack,[e] Robert Bittl,[f] Stergios Piligkos,[a] Høgni Weihe,[a] Philip Tregenna-Piggott,[‡,g] Oliver Waldmann,*[c] and Jesper Bendix*[a]

[a] *Department of Chemistry, University of Copenhagen, Universitetsparken 5 DK-2100 Copenhagen, Denmark. Fax: +45 353 20212; Tel: +45 353 20129; E-mail: ksp@kiku.dk (K.S.P.), bendix@kiku.dk (J.B.)*
[b] *Swiss Light Source, Paul Scherrer Institut, CH-5232 Villigen PSI, Switzerland. E-mail: jan.dreiser@psi.ch*
[c] *Physikalisches Institut, Universität Freiburg, D-79104 Freiburg, Germany. E-mail: oliver.waldmann@physik.uni-freiburg.de*
[d] *Institut für Silizium-Photovoltaik, Helmholtz-Zentrum Berlin, D-12489 Berlin, Germany*
[e] *Institut für Methoden und Instrumente der Forschung mit Synchrotronstrahlung, Helmholtz-Zentrum Berlin, D-12489 Berlin, Germany*
f Institut für Physik, Freie Universität Berlin, D-10115 Berlin, Germany.
[g] *Laboratory for Neutron Scattering, Paul Scherrer Institut, 5232 Villigen PSI, Switzerland.*

Synthesis

$(PPh_4)_3[Ru(CN)_6]$[1] (200 mg, 0.16 mmol) was stirred with NEt_4ClO_4 (120 mg, 0.47 mmol) in MeOH (15 ml) for 10 min. The filtered solution was cooled to –18 °C and filtered again. The pale, yellow solution was added to a cold, filtered solution of [Mn(5-Brsalen)(MeOH)]ClO_4 (100 mg, 0.16 mmol) in MeOH (10 ml). The solution was left in the freezer (–18 °C) overnight to give dark-brown, block-shaped crystals of **1** (50 mg, 44% based on Mn). Anal. calcd (found) for $H_{52}C_{48}N_{11}O_6Mn_2Br_4Ru$: C, 40.90% (40.93%); H, 3.72% (3.54%); N, 10.93% (10.65%).

[1] Prepared analogously to the $AsPh_4^+$ salt, see J. Bendix, P. Steenberg and I. Søtofte, *Inorg. Chem.*, 2003, **42**, 4510-4512.

X-ray crystallography

Single-crystal X-ray diffraction data were collected at 122(1) K on a Nonius KappaCCD area-detector diffractometer, equipped with an Oxford Cryostreams low-temperature device, using graphite-monochromated Mo Kα radiation (λ = 0.71073 Å). The structure was solved using direct methods (SHELXS97) and refined using the SHELXL97 software package.[1] All non-hydrogen atoms were refined anisotropically, hydrogen atoms were located in the difference Fourier map and refined isotropically as constraint riding their parent atom in a fixed geometry. Except for the hydrogen atom (H1) on the MeOH oxygen atom (O1) which hydrogen bonds to cyanide, this hydrogen atom was refined as a free independent atom. Crystal structure and refinement data for 1 are summarized in Table S1. The molecular structure diagrams were made with the Ortep-3 program.[2]
CCDC-806470 contain the supplementary crystallographic data for this paper.

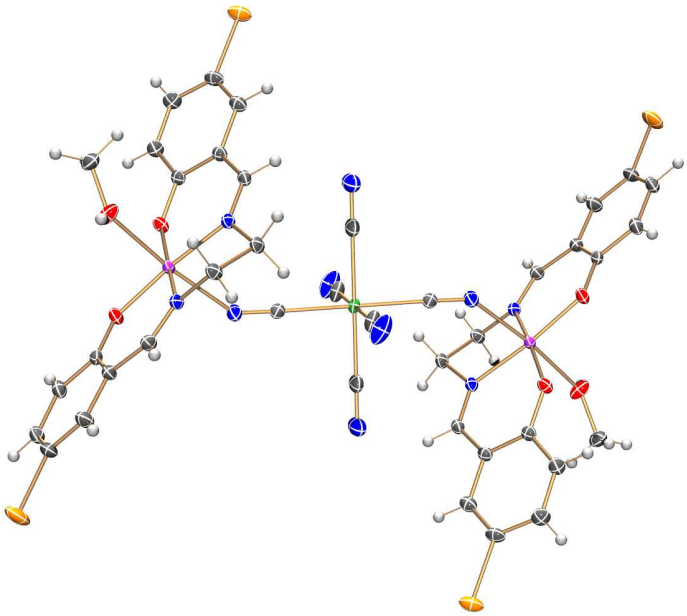

Fig. S1. Molecular structure of 1 drawn at 50% thermal ellipsoid level. The NEt_4^+ counter-ion has been omitted for clarity. Color codes: Mn, purple; Ru, green; O, red; N, blue; C, gray; H, white. Selected bond lengths and angles: Ru–C_{bridge} 2.0447(17) Å; Ru–$C_{non\text{-}bridge}$ 2.049(2) Å, 2.0613(19) Å; C–$N_{CN^-\ bridge}$ 1.156(2) Å; C–$N_{CN^-\ non\text{-}bridge}$ 1.149(3) Å, 1.161 (3) Å; C–Ru–C_{cis} 87.00(7)–93.00(7)°.

[1] G. M. Sheldrick, Acta *Cryst.*, 2008, A64, 112.
[2] L. J. Farrugia, J. Appl. Cryst., 1997, 30, 565.

Table S1 X-ray structure and refinement data for **1**

Chemical formula	$C_{48}H_{52}Br_4Mn_2N_{11}O_6Ru$
Formula Mass	1409.60
Crystal system	Monoclinic
Space group	$P2_1/c$
a/Å	12.3004(16)
b/Å	15.5434(18)
c/Å	15.689(3)
α/°	90.00
β/°	115.318(10)
γ/°	90.00
Unit cell volume/Å^3	2711.5(6)
Temperature/K	122(1)
No. of formula units per unit cell, Z	2
Radiation type	Mo Kα
Absorption coefficient, μ/mm^{-1}	3.738
No. of reflections measured	130903
No. of independent reflections	9444
R_{int}	0.0562
Final R_1 values ($I > 2\sigma(I)$) [a]	0.0277
Final $wR(F^2)$ values ($I > 2\sigma(I)$) [b]	0.0594
Final R_1 values (all data) [a]	0.0416
Final $wR(F^2)$ values (all data) [b]	0.0662
Goodness of fit on F^2	1.117

[a] $R_1 = \Sigma||F_o| - |F_c||/\Sigma|F_o|$. [b] $wR = [\Sigma w(F_o^2 - F_c^2)^2/\Sigma w(F_o^2)^2]^{1/2}$

Selected geometric parameters (Å, °)

Ru—C1	2.0447 (17)	N6—C40^{ii}	1.433 (4)
Ru—C1^{i}	2.0448 (18)	N6—C40	1.433 (4)
Ru—C5	2.049 (2)	N6—C32	1.504 (3)
Ru—C5^{i}	2.049 (2)	N6—C32^{ii}	1.504 (4)
Ru—C4	2.0613 (19)	N6—C42^{ii}	1.573 (4)
Ru—C4^{i}	2.0613 (19)	N6—C42	1.573 (4)
C1—N1	1.156 (2)	N6—C30^{ii}	1.580 (4)
N1—Mn	2.2499 (16)	N6—C30	1.580 (4)
C4—N4	1.161 (3)	N2—C17	1.287 (2)
C5—N5	1.149 (3)	N2—C2	1.472 (2)
Mn—O2	1.8850 (13)	N3—C27	1.285 (2)
Mn—O3	1.8866 (12)	N3—C3	1.480 (2)
Mn—N2	1.9940 (14)	O2—Mn—N2	91.88 (6)
Mn—N3	2.0041 (15)	O3—Mn—N2	173.02 (6)
Mn—O1	2.2380 (14)	O2—Mn—N3	169.86 (6)
C1—Ru—C1^{i}	180.00 (4)	O3—Mn—N3	91.75 (6)
C1—Ru—C5	93.00 (7)	N2—Mn—N3	81.79 (6)
C1^{i}—Ru—C5	87.00 (7)	O2—Mn—O1	88.03 (5)
C1—Ru—C5^{i}	87.00 (7)	O3—Mn—O1	92.23 (6)
C1^{i}—Ru—C5^{i}	93.00 (7)	N2—Mn—O1	89.74 (6)
C5—Ru—C5^{i}	180.0	N3—Mn—O1	84.04 (6)
C1—Ru—C4	89.26 (7)	O2—Mn—N1	91.91 (6)
C1^{i}—Ru—C4	90.74 (7)	O3—Mn—N1	93.84 (6)
C5—Ru—C4	90.44 (8)	N2—Mn—N1	84.18 (6)
C5^{i}—Ru—C4	89.56 (8)	N3—Mn—N1	95.30 (6)
C1—Ru—C4^{i}	90.74 (7)	O1—Mn—N1	173.91 (6)
C1^{i}—Ru—C4^{i}	89.26 (7)	C10—O1—Mn	130.05 (12)
C5—Ru—C4^{i}	89.56 (8)	C10—O1—H1	108 (2)
C5^{i}—Ru—C4^{i}	90.44 (8)	Mn—O1—H1	119 (2)
C4—Ru—C4^{i}	180.0	C17—N2—Mn	126.18 (12)
N1—C1—Ru	175.86 (16)	C2—N2—Mn	112.78 (10)
C1—N1—Mn	144.12 (14)	C11—O2—Mn	128.03 (11)
N4—C4—Ru	179.6 (2)	C27—N3—Mn	126.22 (12)
N5—C5—Ru	177.55 (17)	C3—N3—Mn	113.35 (11)
O2—Mn—O3	94.88 (5)	C21—O3—Mn	129.71 (11)

Symmetry codes: (i) −*x*, −*y*+1, −*z*; (ii) −*x*+1, −*y*, −*z*+1.

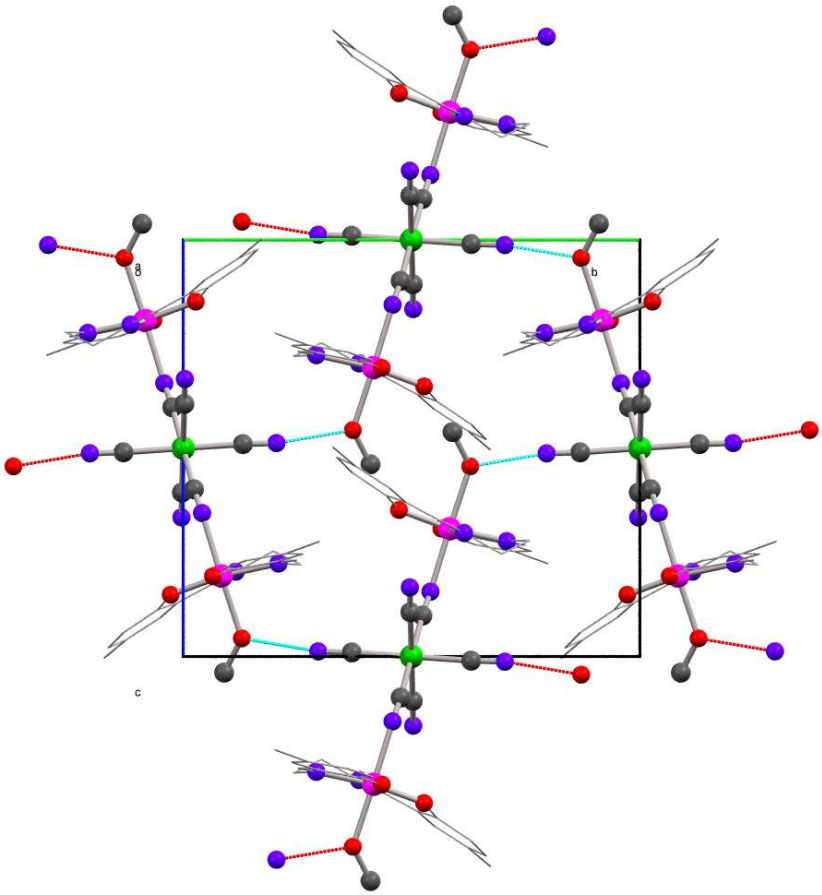

Fig S2. Unit cell along the *a* axis. Hydrogen bonds are drawn in blue. The 5-Brsalen^{2-} ligand is shown as wireframe representation.

Hydrogen-bond geometry (Å, °)

D—H···*A*	*D*—H	H···*A*	*D*···*A*	*D*—H···*A*
O1—H1···N5^{iii}	0.80 (2)	1.90 (2)	2.693 (2)	173 (3)

Symmetry code: (iii) −*x*, *y* − 1/2, −*z* + 1/2.

FDFT THz-EPR measurements

Linearly polarized THz radiation in the range between 5 and 30 cm^{-1} was coupled out from the BESSY storage ring. It was then passed through a FTIR spectrometer with the resolution set to 0.1 cm^{-1} and using a 125 µm-thick beamsplitter. The transmitted intensity was detected by a liquid-Helium cooled bolometer. The powder of **1** (70 mg) was carefully ground and filled into a sample holder with Teflon windows. The sample holder was mounted on a variable-temperature insert inside an opto-magnetic cryostat. The diameter of the cross-section exposed to the beam was ~10 mm. All measurements reported here were performed on the powder sample.

FDFT THz-EPR transmission spectra were calculated using full diagonalization of the Hamiltonian Eq. 1 with the parameters given in the main text. The calculated absorbance spectra shown in Fig. 3 of the main text take into account the reference at 25 K, which can lead to a negative "absorbance" at low temperatures for "warm" peaks, i.e. peaks that arise from transitions between excited states.

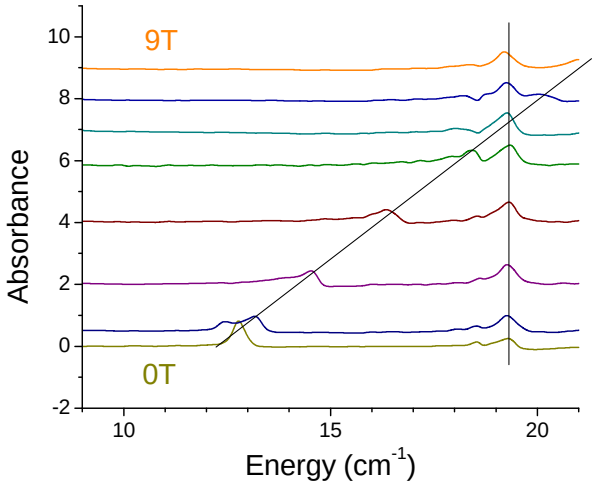

Fig. S3. Coarse *B* field dependence at 5 K with fields indicated in the plot. The black solid lines are guides to the eye. The curves were offset by 1 unit per 1 T.

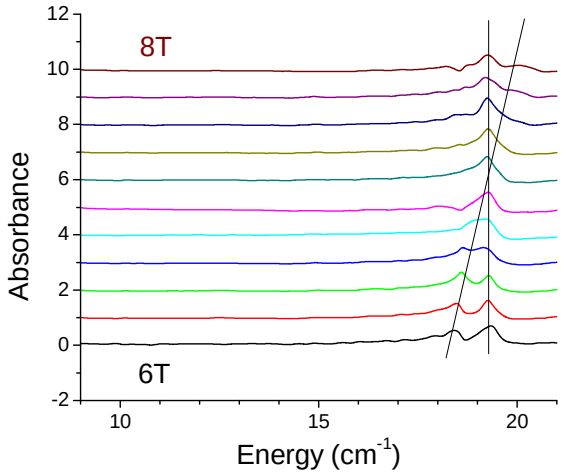

Fig. S4. Fine *B* field dependence at 5 K in the vicinity of the crossing of M1 and P2. The black solid lines are guides to the eye. The curves were offset by 1 unit per 200 mT.

Magnetic measurements

The magnetic measurements were conducted on a Quantum-Design™ MPMS-XL SQUID magnetometer located at the University of Copenhagen. The susceptibilities (H_{dc} = 1 kOe) were corrected for diamagnetic contributions from the sample holder and the sample (estimated from Pascal's constants). The polycrystalline sample was immobilized in frozen *n*-eicosane to prevent orientation effects. Ac susceptibility measurements were measured with various frequencies in the range 50–1500 Hz with an ac field amplitude of 3.8 Oe with and without an applied static field.

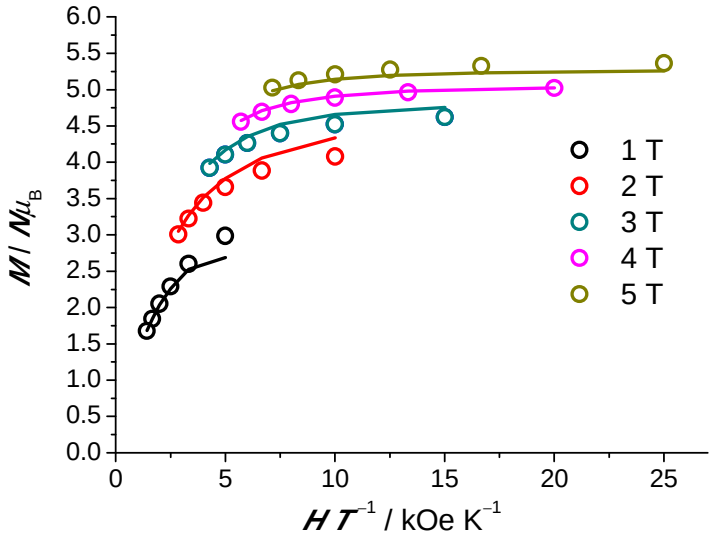

Fig. S5. Reduced magnetisation. Circles correspond to experimental data and lines represent simulations using the best-fit parameters mentioned in the text.

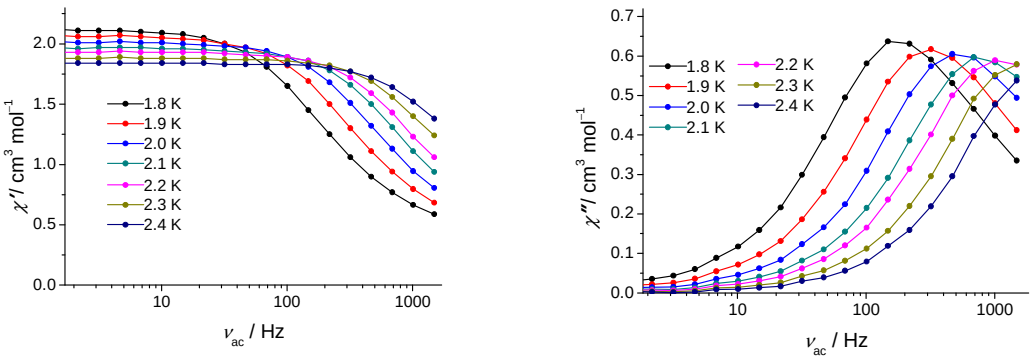

Fig. S6. In-phase (left) and out-of-phase (right) components of the ac susceptibility in the absence of a dc field. Solid lines are guides for the eyes.

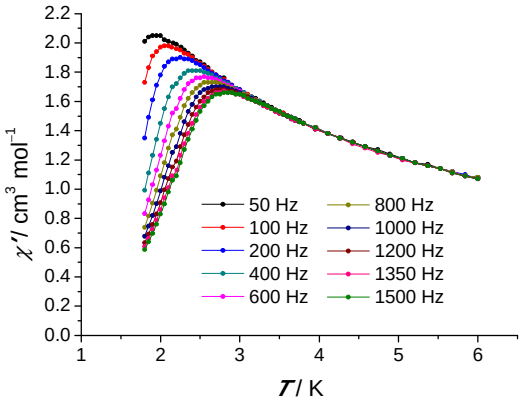

Fig. S7. In-phase component of the ac susceptibility in the absence of a static field. Solid lines are guides for the eyes.

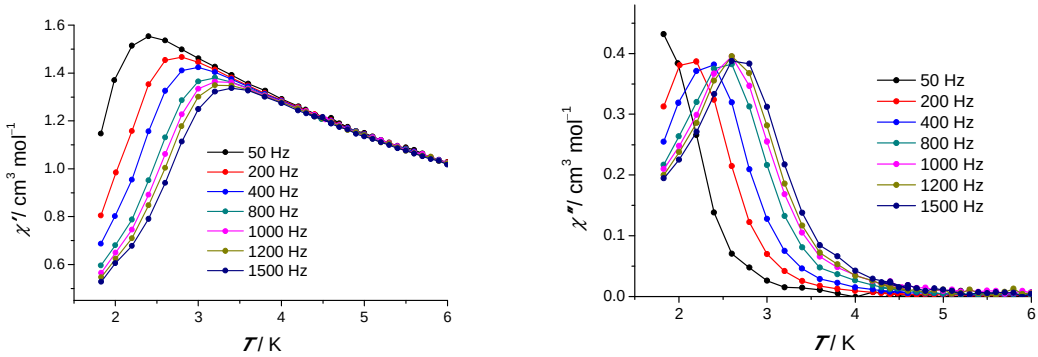

Fig. S8. In-phase (left) and out-of-phase (right) components of the ac susceptibility in an applied dc field of 4 kOe. Solid lines are guides for the eyes.

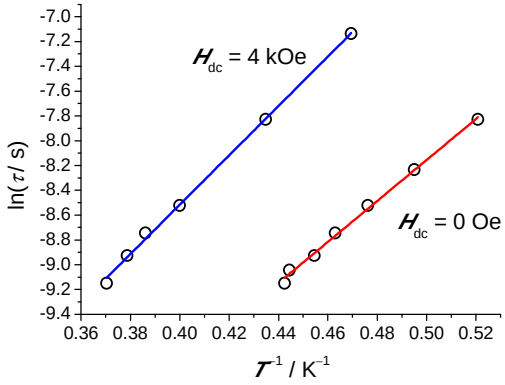

Fig. S9. Arrhenius plot obtained from the peak positions of the $\chi''(T)$ by assuming $\tau(T) = \omega^{-1}$ (where $\omega = 2\pi\nu_{ac}$)

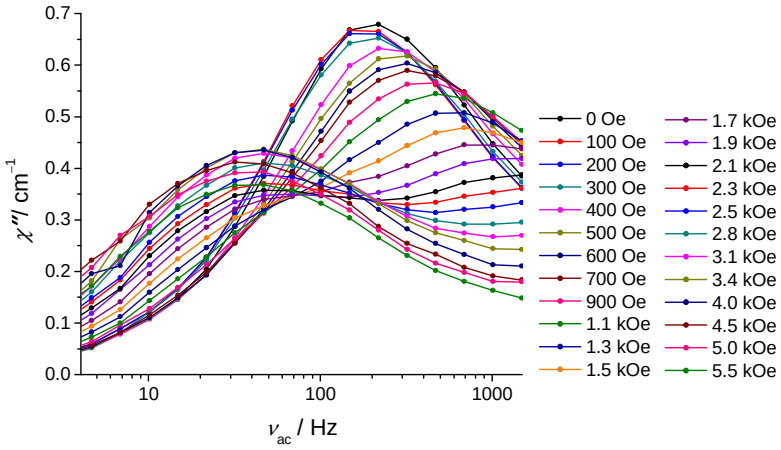

Fig. S10. Field dependence of $\chi''(\nu_{ac})$ at T = 1.8 K.

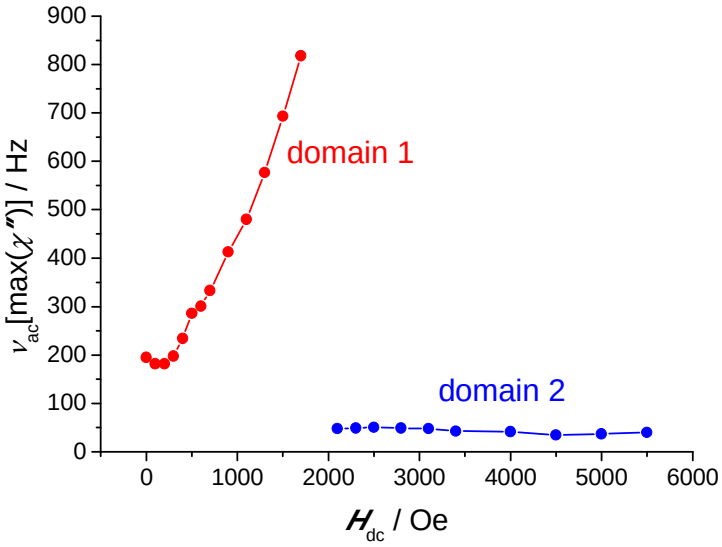

Fig. S11. Field dependence of the characteristic frequency extracted from the peak maxima of Fig. S10.